buildings

MDPI

Article

An Investigation of Key Mechanical and Physical Characteristics of Geopolymer Composites for Sustainable Road Infrastructure Applications

Adam Kmiotek [1], Beata Figiela [1], Michał Łach [1,2], Lyazat Aruova [3] and Kinga Korniejenko [1,2,*]

[1] Faculty of Materials Engineering and Physics, Cracow University of Technology, 37 Jana Pawła II Street, 31-864 Cracow, Poland; adam.kmiotek@student.pk.edu.pl (A.K.); beata.figiela1@pk.edu.pl (B.F.); michal.lach@pk.edu.pl (M.Ł.)
[2] Interdisciplinary Center for Circular Economy, Cracow University of Technology, Warszawska 24, 31-155 Cracow, Poland
[3] Faculty of Architecture and Civil Engineering, Gumilyov Eurasian National University, Kazhymukan Str. 13, r205, Astana 010008, Kazakhstan; ecoeducation@mail.ru
* Correspondence: kinga.korniejenko@pk.edu.pl; Tel.: +48-609974988

Abstract: One of the most important areas of the construction industry is road infrastructure. It plays a crucial role in the economy of various countries. Today's roads must withstand long-term temperature and load differences, but some of the infrastructure cannot survive these tests, and after one severe winter, there may be asphalt cracks and holes that need to be repaired. This problem requires new applications and more resistant materials. Geopolymers are potential candidates. This class of material as a building material for roads has the potential to withstand frost and salt. The aim of the study herein is to demonstrate the mechanical and physical properties of a composite geopolymer made from fly ash, coal shale, nanosilica, and carbon fiber for potential application in road infrastructure. The research and experiments herein will serve to determine whether geopolymers are suitable for replacing traditional concrete in road construction processes. The following research methods were applied: SEM, XRF, XRD, compressive strength testing, abrasion, and investigation of freeze–thaw resistance in a climatic chamber. The results confirm the potential possibility of applying geopolymer compositions in road infrastructure, including sufficient mechanical properties such as ca. 38 MPa and freeze–thaw resistance, as shown by mass loss of about 1.7%, as well as sufficient abrasion resistance, as shown by mass loss of about 4%.

Keywords: geopolymer; sustainable road infrastructure; mechanical properties

Academic Editor: Huayang Yu

Received: 1 March 2025
Revised: 2 April 2025
Accepted: 9 April 2025
Published: 11 April 2025

Citation: Kmiotek, A.; Figiela, B.; Łach, M.; Aruova, L.; Korniejenko, K. An Investigation of Key Mechanical and Physical Characteristics of Geopolymer Composites for Sustainable Road Infrastructure Applications. *Buildings* **2025**, *15*, 1262. https://doi.org/10.3390/buildings15081262

1. Introduction

More and more stringent regulations regarding ecological solutions are forcing us to move away from traditional concrete; in the production of concrete, a ton of CO_2 is produced from each ton of raw material produced [1,2]. The possible solutions are associated with the replacement of a part of traditional concrete with waste or industrial by-products, as well as the design of alternative materials such as geopolymers [3,4]. The second approach seems to be a more long-term approach to solving this problem. Geopolymers are the ecological alternative in construction to traditional cement, which is usually ordinary Portland cement [5,6]. One of the most important areas of construction is road infrastructure; a large part of the economy of various countries is based on it. Because of this, even partly replacing traditional materials with more ecological ones can

bring about large-scale effects. Today's roads have to not only fulfill strength requirements but must also withstand long-term temperature and load differences; some infrastructure cannot withstand these tests, and after one severe winter, asphalt cracks and holes may need to be repaired. This kind of construction also has to withstand frost and salt, which would prevent construction in many countries [7,8].

Previous investigations have shown the possibility of applying geopolymers as a material for road construction, including the application of industrial by-products such as fly ash or slag for material preparation [9,10]. Particular attention should be paid to the use of local waste for this purpose in order to limit the cost of transportation and the pollution connected to them. However, the implementation of such waste products seems very attractive; it has to be stressed that different waste streams have slightly different characteristics depending on local conditions, and because of that, they require additional research before application [11,12]. In some use cases, such kinds of waste, alongside computer methods, can play an important role in the optimization of geopolymers' composition [13].

Another important factor is obtaining proper compositions of used materials, which should include the prevention of cracking. One of the most popular methods of avoiding this phenomenon is the addition of fibers. Most previous research confirms the possibility of the application of different fibers for this purpose [14,15]. In this case, the best results are obtained by using carbon fibers. They not only prevent cracking but also do not influence compressive strength and enhance the flexural strength and fracture tongues of materials [16–18]. When steel fibers are used, they are not harmful in the case of material surface degradation, for example, as a result of surface abrasion.

In recent years, micro- and nano-additives have also emerged as points of interest for scientists, as a potential admixture to compositions made especially for roads [8]. Even a small amount of this additive can significantly affect the properties of the material. Currently, mineral nano-additives, such as nano-silica and nano-clays, are the most intensively researched solutions used in road construction, especially if we consider concrete applications [8,19,20]. The other popular group is that of metal compounds [8,21]. Both metals and ceramics may be classified into one group of inorganic nano-additives. The addition of nanoparticles to this group could have different purposes. The most common are catalytic applications [22]; enhancement of the physical and rheological properties, including the increased durability of asphalt mixtures [21,23]; improved rutting resistance [24]; fatigue properties; and temperature resistance [24,25]. Despite a lot of benefits, the usage of nano-additives also brings some challenges. In the case of inorganic ones, the basic issue is their poor affinity to the organic materials used in road composition [26,27]. In the case of geopolymers (inorganic compounds), this problem does not appear.

Despite a relatively large amount of research in the field of geopolymers with nano-additives, geopolymer nanocomposites have not been widely investigated with the intention of applying them in the road industry. However, other investigations into geopolymers with nano-additives have shown their potential as a construction material, including some pavement technologies. Among others, one promising additive seems to be nano-silica, and research works have shown its potential to improve the mechanical properties of geopolymers. Previous works have shown that it enhances mechanical and rheological properties [28–30], resistance to sulfate attack [31], durability [32], and thermal resistance [33,34]. In the case of metal and metal oxide nanoparticles, investigations have focused mainly on the addition of titanium dioxide and photocatalytic properties [35]. Other types of compounds have been investigated in the area of antimicrobial properties and improving compressive strength [33,36].

The literature gap shows the necessity of designing more complex materials for road construction. The main motivation for the choice of this topic stemmed from questions

regarding the feasibility, economic viability, and environmental impact of using geopolymers compared to traditional concrete. This article presents the process of research and experiments carried out to confirm the suitability of geopolymers for road infrastructure. The aim of the work was to determine the possibility of using geopolymer composites as materials for road infrastructure. The work included the synthesis of geopolymer materials and the examination of selected mechanical and physical properties.

2. Materials and Methods

2.1. Materials

For the geopolymer sample preparation, the following ingredients were used: fly ash from a power plant Skawina (CHP Skawina, Skawina, Poland); coal shale—a by-product from mining from the Silesia mine (Silesia mine, Czechowice-Dziedzice, Poland); short carbon fibers—3 mm (R&G GmbH, Waldenbuch, Germany); and nano-silica (Nanografi Nano Technology, Ankara, Turkey). The additives were selected to improve the material properties required for road application and give a synergic effect [37]. Fly ash, carbon fiber, and nano-silica were used in an unaltered state. The coal shale, before its usage, was calcinated to improve its reactivity during geopolymer synthesis. At first, the coal shale was crushed, ground, and sifted through a special sieve to separate it from larger unground items. Then, the material was processed by calcination (a thermal activation) to remove carbon residues and achieve appropriate reactive microstructures. This process took place at a temperature of 800 °C for 24 h. In the next step, the material was characterized according to its chemical and mineralogical composition as well as its microstructure.

2.2. Raw Material Analysis

2.2.1. Fly Ash

In the first step, the elemental and oxide compositions were investigated to confirm the suitability of the material for the geopolymerization process, as shown in Tables 1 and 2.

Table 1. Elemental analysis of the used raw materials.

Element	Fly Ash	Coal Shale	Nano-Silica
Si	44.331%	43.476%	99.760%
Al	20.016%	20.677%	---
Fe	16.526%	22.448%	0.009%
K	7.448%	6.250%	---
Ca	7.364%	2.146%	---
Ti	2.119%	1.776%	0.005%
S	1.109%	1.460%	0.126%
Mn	0.236%	0.208%	0.019%
Sr	0.229%	0.087%	---
V	0.192%	0.158%	---
Zn	0.094%	0.089%	0.001%
Zr	0.082%	0.058%	---
Cu	0.051%	0.068%	0.008%
Ni	0.031%	0.164%	---
Others	0.172%	0.075%	0.072%

The elemental composition of fly ash showed the content of the typical elements such as silicon and aluminum. The analyzed fly ash also included an amount of iron (above 16%) and other elements, such as potassium, calcium, titanium, and sulfur. This composition is typical of fly ash from the energy industry [38].

Table 2. Oxide analysis of used raw materials.

Oxide	Fly Ash	Coal Shale	Nano-Silica
SiO_2	53.525%	51.875%	99.863%
Al_2O_3	24.866%	24.891%	---
Fe_2O_3	9.360%	13.896%	0.002%
CaO	4.576%	1.599%	0.004%
K_2O	4.217%	3.490%	---
TiO_2	1.506%	1.352%	---
SO_3	1.395%	1.755%	0.074%
P_2O_5	---	0.447%	---
V_2O_5	0.127%	0.126%	---
MnO	0.122%	0.119%	---
SrO	0.091%	0.038%	---
ZnO	0.040%	0.040%	0.001%
ZrO_2	0.037%	0.029%	---
Cr_2O_3	0.037%	0.220%	0.006%
CuO	0.022%	0.035%	0.003%
NiO	---	0.031%	---
Others	0.086%	0.055%	0.048%

Figure 1 presents the results of the investigation of the mineral composition of the fly ash. The presented fly ash fulfilled the requirements for fly ash class F, following ASTM C618, including a CaO value of 4.576% (<10%), a total SiO_2 + Al_2O_3+ Fe_2O_3 value of 87.751% (>70%) and SO_3 of 1.395% (<5%) [39]. This kind of fly ash is suitable for geopolymerization processes and should create a proper material structure [11,40].

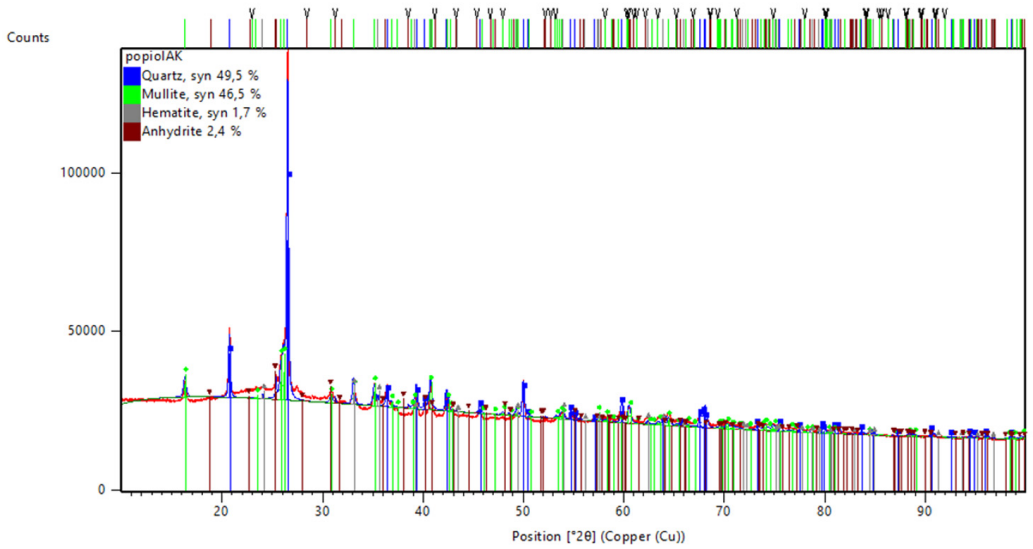

Figure 1. XRD patterns for fly ash.

The presented pattern shows that among the crystalline ingredients of fly ash, the main mineralogical components are quartz (49.5%) and mullite (46.5%). The quartz does not influence the reactivity of the material, but in the final composition, it allows the required strength to be obtained [41]. Mullite is also hardly reactive; it reacts with alkaline solutions to a limited degree [42]. However, mullite, similar to quartz, can ensure that the final products have enhanced strength and durability [43,44]. XRD analysis shows a small amount of hematite (1.7%) and anhydrite (2.4%).

SEM observations for the material are presented in Figure 2.

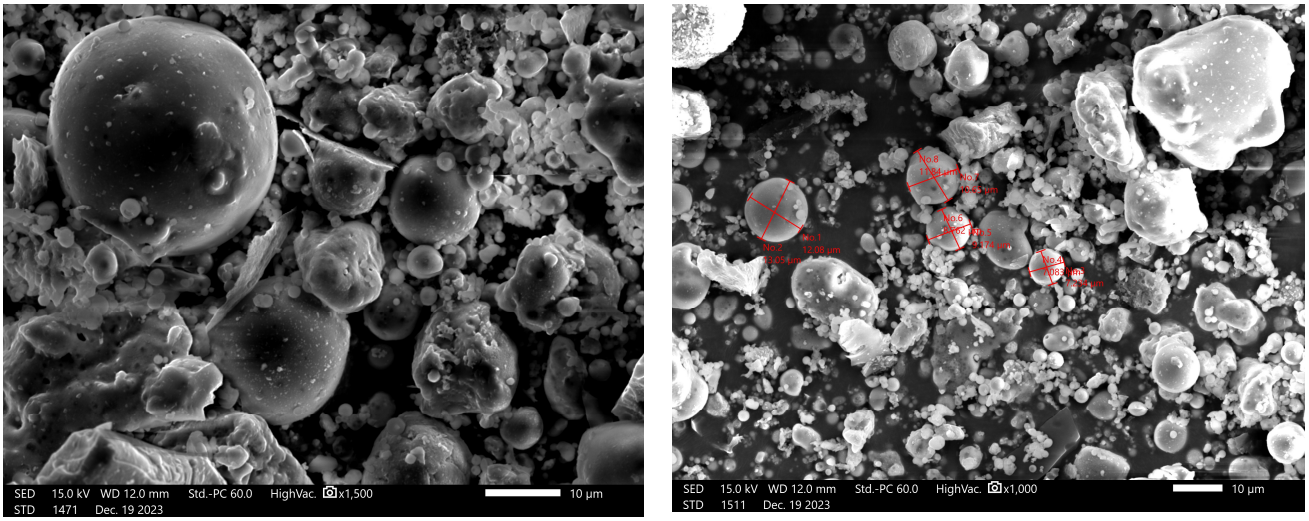

(**a**) (**b**)

Figure 2. SEM images of fly ash: (**a**) magnification 1500×; (**b**) magnification 1000× with marked selected particles sizes.

Fly ash is characterized by the presence of many spherical particles. This kind of particle usually gives the fresh paste good workability and allows the amount of water used to be reduced [45].

2.2.2. Coal Shale

According to the data presented in Table 1, coal shale is mainly composed of silicon, aluminum, and iron. It also includes other elements, such as potassium, calcium, titanium, and sulfur. Table 2 shows the oxide composition. The main component in this case is SiO_2. In the material, there is also a significant amount of Al_2O_3 and Fe_2O_3. All of these elements are supportive of a geopolymerization reaction.

Figure 3 presents the results of the investigation of the mineral composition of coal shale "Silezia" after the calcination process.

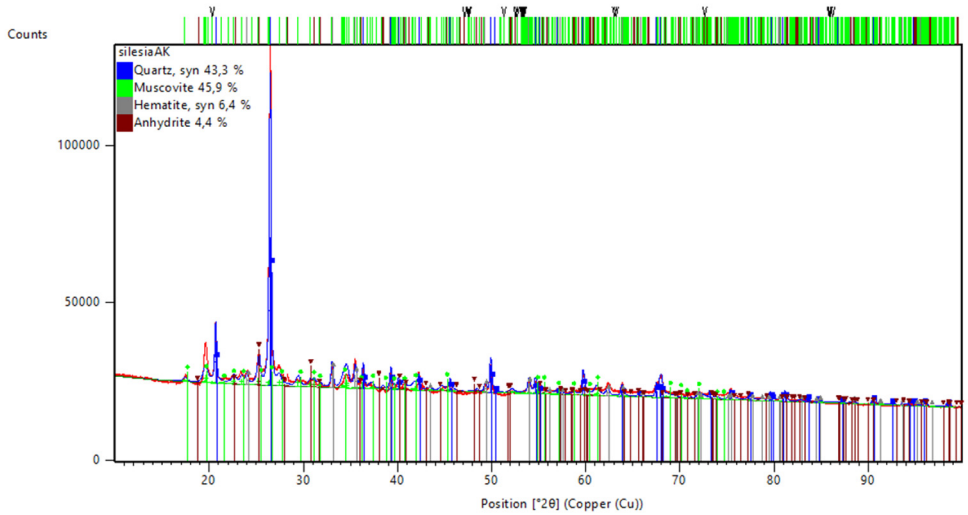

Figure 3. XRD patterns for coal shale "Silezia".

The presented pattern shows the crystalline ingredients of the milled coal shale "Silezia". The main component is quartz, with 43.3%, followed by muscovite, with 45.9%. The quartz, just as in the case of the fly ash, plays the role of filler in the material, allowing the required strength of the final composition to be obtained [41]. Muscovite is only partly

reactive and can be challenging when trying to obtain a proper geopolymer microstructure, in comparison with kaolinite, even after calcination [46]. However, when this mineral is present, the geopolymerization process at a temperature above 70 °C seems to be important for the efficiency of the process, as well as ensuring a high pH value [46–48]. XRD analysis shows a certain amount of hematite (6.4%) and anhydrite (4.4%). The presence of these minerals is higher than in fly ash, but still not very high. The lack of kaolinite in the analysis is caused by its change into an amorphous phase, becoming metakaolin after the calcination process. This mineral normally appears in coal shale [40,49].

SEM observations of the material are presented in Figure 4.

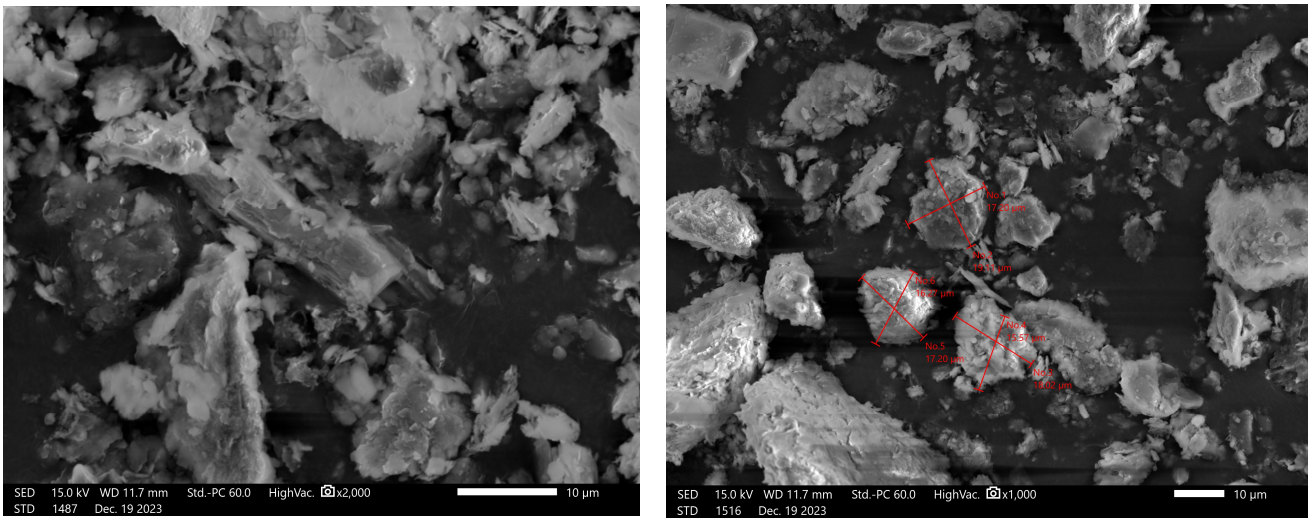

(**a**) (**b**)

Figure 4. SEM images of coal shale: (**a**) magnification 2000×; (**b**) magnification 1000× with marked selected particles sizes.

The microstructure investigation in the case of coal shale shows sharp elements with irregular shapes, which are an effect of grinding the material.

2.2.3. Nano-Silica

According to the data presented in Tables 1 and 2, nano-silica is mainly composed of SiO_2, which is also confirmed by the XRD analysis in Figure 5.

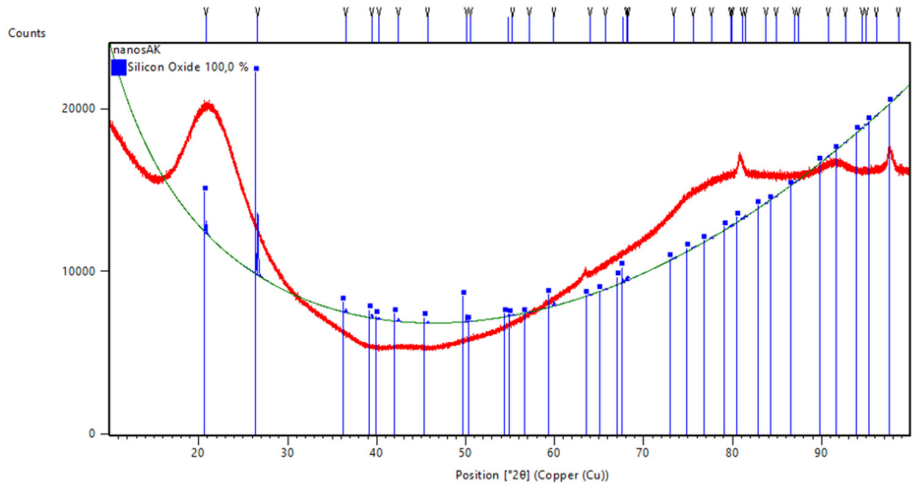

Figure 5. XRD patterns for nano-silica. The red line is a result of the invastigation (the same as on the previous patterns). Other colors are supportive lines generated by the program to show different phases. The green one is just a shape and the blue ones are market peaks for the phase.

Silicon oxide is an ingredient of nano-silica. The material has a highly amorphous character. SEM observations of the material are presented in Figure 6.

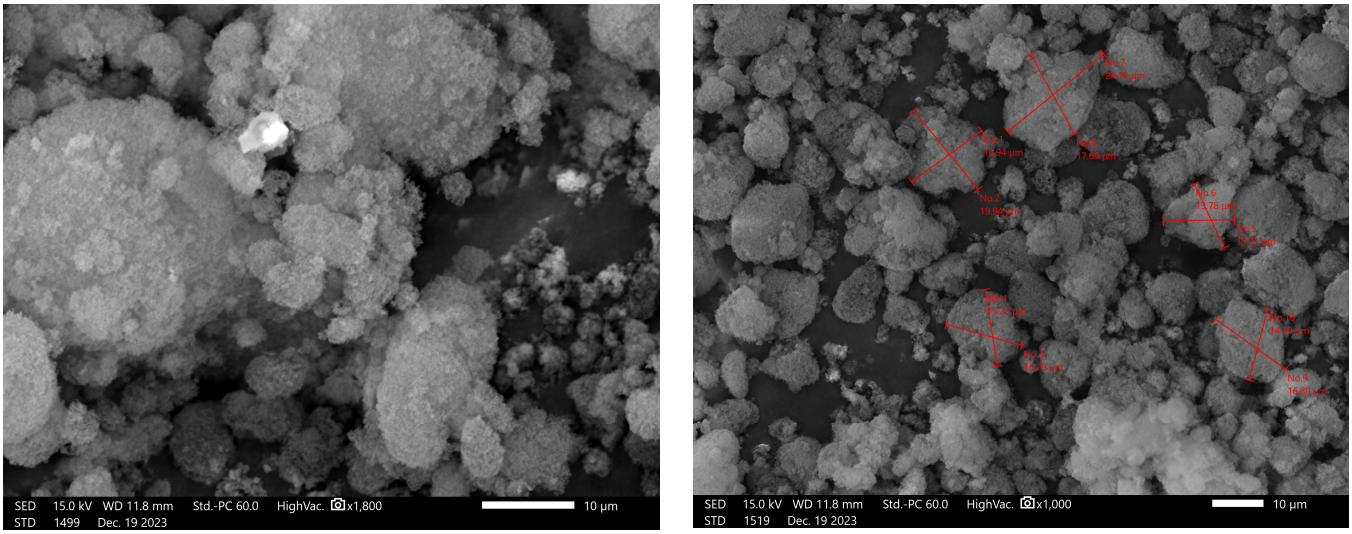

(**a**) (**b**)

Figure 6. SEM images of nano-silica: (**a**) magnification 1800×; (**b**) magnification 1000× with marked selected particles sizes.

The nano-silica has particles of a regular shape; the small particles are very often agglomerated into larger clusters, which is more visible with higher magnification. To work effectively, nano-silica should be divided into smaller particles to be effectively integrated into the geopolymer matrix.

2.2.4. Carbon Fibers

For the carbon fibers, SEM observations are presented in Figure 7.

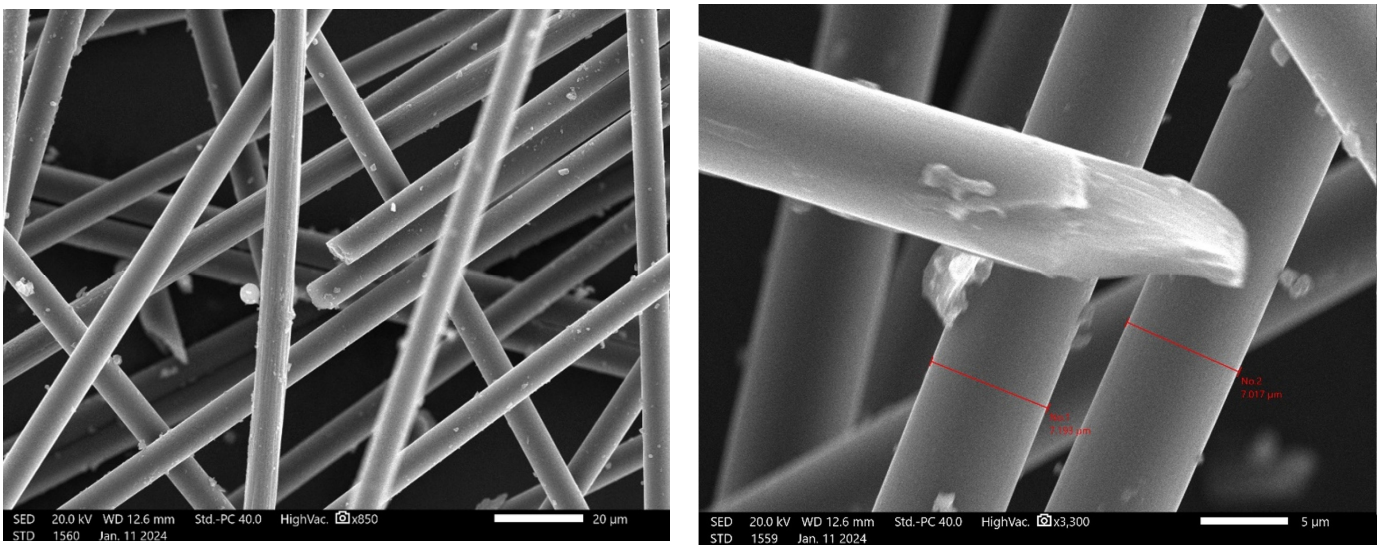

(**a**) (**b**)

Figure 7. SEM images of carbon fibers: (**a**) magnification 850×; (**b**) magnification 3300× with marked selected fibers' diameters.

SEM investigation confirmed the regular character of the fibers. The measurements show that they all have a diameter of about 7 µm and smooth surfaces.

2.3. Samples Preparation

The day before the samples' preparation, a 10 molar solution of a mixture of hydrated sodium hydroxide flakes with aqueous sodium silicate type R-145 (molar module 2.5, density 1.45 g/cm^3) in a ratio of 1:2.5 was synthesized. It was stored in laboratory conditions to equalize the concentrations. Next, the samples were made. To prepare the samples, the dry ingredients of the mass were combined (Table 3), and then an alkaline solution was added to them.

Table 3. Sample composition.

Sample	Fly Ash [g]	Coal Gangue from Silesia Mine [g]	Carbon Fiber [g]	Nano-Silica [g]	Solution 10M [g]
Reference sample (REF)	2344	-	-	-	930
Geopolymer composite (GP)	2000	320	16	8	930

The geopolymer composite was made based on FA with the addition of coal gangue, carbon fibers, and nano-silica. Each component was planned for the improvement of material properties. The role of coal gangue was the reinforcement of mechanical properties and lowering costs by using industrial by-products. CFs should enhance flexural strength and work against cracking in changeable preparations. Nano-silica should also improve physical and mechanical properties, including resistance against friction and limited water absorption. The reference sample was created based on FA to compare if the above additions brought about the expected effects.

The mass prepared in this way was mixed in a special laboratory mixer for 10 min. After this time, the geopolymer mass was transferred to appropriate forms, and the molds were placed on a vibrating table to remove air bubbles. The scheme of the samples' preparation is presented in Figure 8.

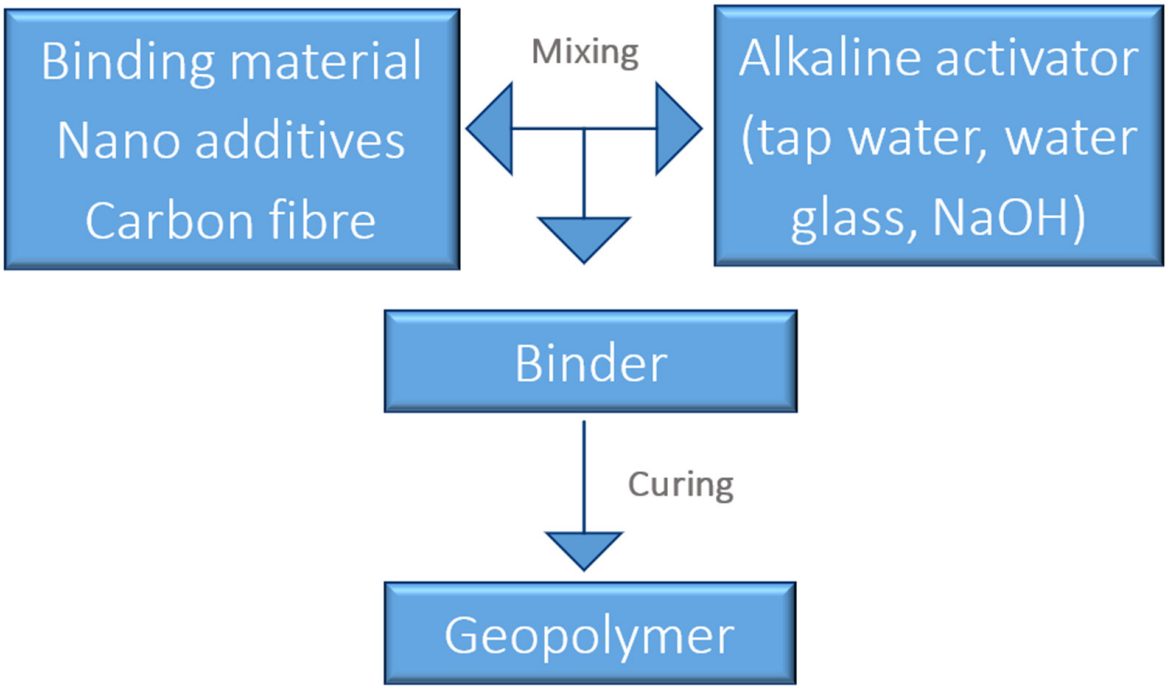

Figure 8. Scheme of samples' preparation.

Then, the samples were placed in the oven for 24 h at 75 °C. The time was due to the laboratory's schedule, and the setting time was between 8 and 12 h. The next day, they were unmolded and left in laboratory conditions for development for 28 days.

2.4. Methods

The elemental and oxide composition were investigated by X-ray fluorescence (XRF). The research was performed using the EDX-7200 from the company SHIMADZU (SHIMADZU EUROPA GmbH, Duisburg, Germany) and the software PCEDX Navi (Version: EDX-7000P). The materials were powdered, put into plastic, and covered by polypropylene foil. They were measured in an air atmosphere.

The mineralogical composition was measured by X-ray diffraction (XRD). The measurements were made using AERIS from the company Malvern PANalytical (PANalytical, Almelo, The Netherlands). The test was performed using a copper lamp. The detailed parameters of the machine's settings were as follows: starting and ending angle—9.999–100 °2 θ; measurement step—0.0027166 °2 θ; time for measurement—340.425 s; total testing time—13 h 2 min 32 s; nickel filter; a 13 mm mask; knife in the low position; and a 1 mm gap. The measurements were made using powdered samples.

To study the microstructure, a JSM-IT200 InTouchScope™ scanning electron microscope (JEOL, Tokyo, Japan) was used. The samples were placed in a pot using carbon tape and covered by a gold layer to obtain conductivity. The observations were made at different magnifications; additionally, an automatic virtual ruler was involved in checking the grains' dimensions.

Density was measured by using the geometric method by employing a caterpillar and laboratory weight. The test involved three samples of each type.

The compressive strength test was performed using MATEST (Matest, Treviolo, Italy). The test was provided according to the standard PN-EN 12390-3:2019 for the testing of concrete—Part 3: the Compressive strength of test specimens [50]. Samples with dimensions of 50 mm × 50 mm × 50 mm were used for this test. The test involved three samples of each type.

The abrasion resistance was investigated using a Böhme disk (Matest, Treviolo, Italy). The main element of this device is an iron horizontal disc with a diameter of 750 mm and a 200 mm test track used to position specimens. The maximum speed of rotation was 30 rpm. The initial force was 294 ± 3 N on the specimen. The test consisted of abrading the sample surface using corundum powder (20 g of artificial corundum for each cycle). A single cycle consisted of 22 revolutions of the Böhme dial. Abrasion wear was measured after 16 cycles on each sample, and after each cycle, the sample was rotated 90° to ensure uniform abrasion in all directions. The samples used for the test were cubes of 50 mm × 50 mm × 50 mm. The sample height and weight were determined before and after the test. The test involved three samples of each type.

This process of investigating freeze–thaw resistance intended to examine the percentage of each sample's weight loss over cycles of freezing and thawing (as a simulation of changeable temperature during the year in countries such as Poland and Kazakhstan) in a climatic chamber (WeissTechnik GMbH, Reiskirchen-Lindenstruth, Germany). Before starting the study, the samples were weighed; their weight was recorded, and then they were transferred to a chamber where they were exposed to cycles of temperature changes from −40 °C to 80 °C (Table 1). Samples were tested in such cycles for 24 h. Each cycle lasted 90 min, which translates into 16 cycles per day, as shown in Table 4.

The entire study took 36 days. This value was estimated taking into consideration the predicted lifetime of the material for the road (10 years) and the number of days with a transition to 0 °C in Poland (57) [51].

Table 4. The basic parameters of investigation in a climatic chamber.

Step	Time [min]	T [°C]
temperature stabilization	0	23
holding temperature	15	−40
heating	30	up to 80
holding temperature	15	80
cooling	30	up to −40

3. Results

3.1. Density

The results of the density measurements are presented in Table 5.

Table 5. Density.

Sample	Weight [g]	Volume [g/cm^3]	Density [g/cm^3]
REF	232.04	129.47	1.78
GP	205.25	132.9	1.53

The additives allowed for a reduction in the weight of the composition. This weight reduction is desirable if it does not significantly affect mechanical properties [52,53]. In the case of building materials, a reduction in weight is connected with a decrease in the cost of transportation and CO_2 emissions [54,55].

3.2. Mechanical Properties—Abrasion and Compressive Strength

The results of compressive strength are presented in Table 6.

Table 6. Compressive strength.

Sample	Compressive Strength [MPa]	Standard Deviation [MPa]
REF	34.90	7.80
GP	37.70	8.19

Compressive strength is a basic parameter for cementitious materials. The investigated composition obtained very good compression strength, taking into consideration that they it was a paste without aggregates. The compressive strength was almost 35 MPa for the reference sample and almost 38 MPa for the reference sample. The minimum requirement for bicycle paths, sidewalks, and forest roads is 30 MPa [56]. The addition of fine aggregate or coarse aggregate can increase this value within the composition.

Additionally, the abrasion resistance was tested, as shown in Table 7.

Table 7. Abrasion resistance of geopolymer composites.

Sample	Weight Before Test	Weight After Test	% Change
REF	232.04	221.63	4.48
GP	205.25	196.87	4.08

The additives improved the abrasion resistance of the geopolymers. Compared to reference samples, a lower mass loss was noted. These properties are important for road applications, especially to ensure the proper durability, fatigue performance, rutting resistance, and wear resistance of the composition [57,58].

3.3. Freeze–Thaw Resistance and Visual Assessment

The results of the investigation of freeze–thaw resistance are presented in Table 8.

Table 8. Freeze–thaw resistance of geopolymer composites in a climatic chamber.

Sample	Weight Before Test	Weight After Test	% Change
REF	209.99	206.10	1.85
GP	204.01	200.52	1.71

The additives enhanced the freeze–thaw resistance of the geopolymers. The obtained results show good resistance against conditions typical of many countries in central Europe and central Asia. The most important ingredient that plays a role in the improvement of this property is nano-silica. Another investigation confirmed their influence on freeze–thaw resistance [32]. The mechanics reinforced by fibers may also be responsible for better material coherence, especially the prevention of the propagation of microcracks in the material [56].

Additionally, some visual observations of selected samples were made after the friction test. They were half-submerged in the water and were sprinkled with road salt. The main aim of this experiment was to visually assess any changes in possible conditions during the late autumn or early spring season in temperate climates, where salt is commonly used as a medium to counteract ice on the road (Figure 9).

(**a**) (**b**)

Figure 9. Sample of geopolymer composition sprinkled with road salt: (**a**) after 1-week exposition; (**b**) after 1-month exposition.

After 1 week, no significant changes were noted. The salt did not significantly influence the structure of the material. Most of the salt was left in solid form; only a small amount was dissolved (Figure 9a). After 1 month, visible efflorescence appeared on the material. This phenomenon can also occur in geopolymers without the presence of salt [59]. It did not significantly influence the salt's behavior (Figure 9b). In both cases, there was a lack of reaction between the geopolymer composites and salt.

3.4. Microstructure Investigation

Microstructural analysis of the geopolymer composites was performed using SEM, as shown in Figure 10.

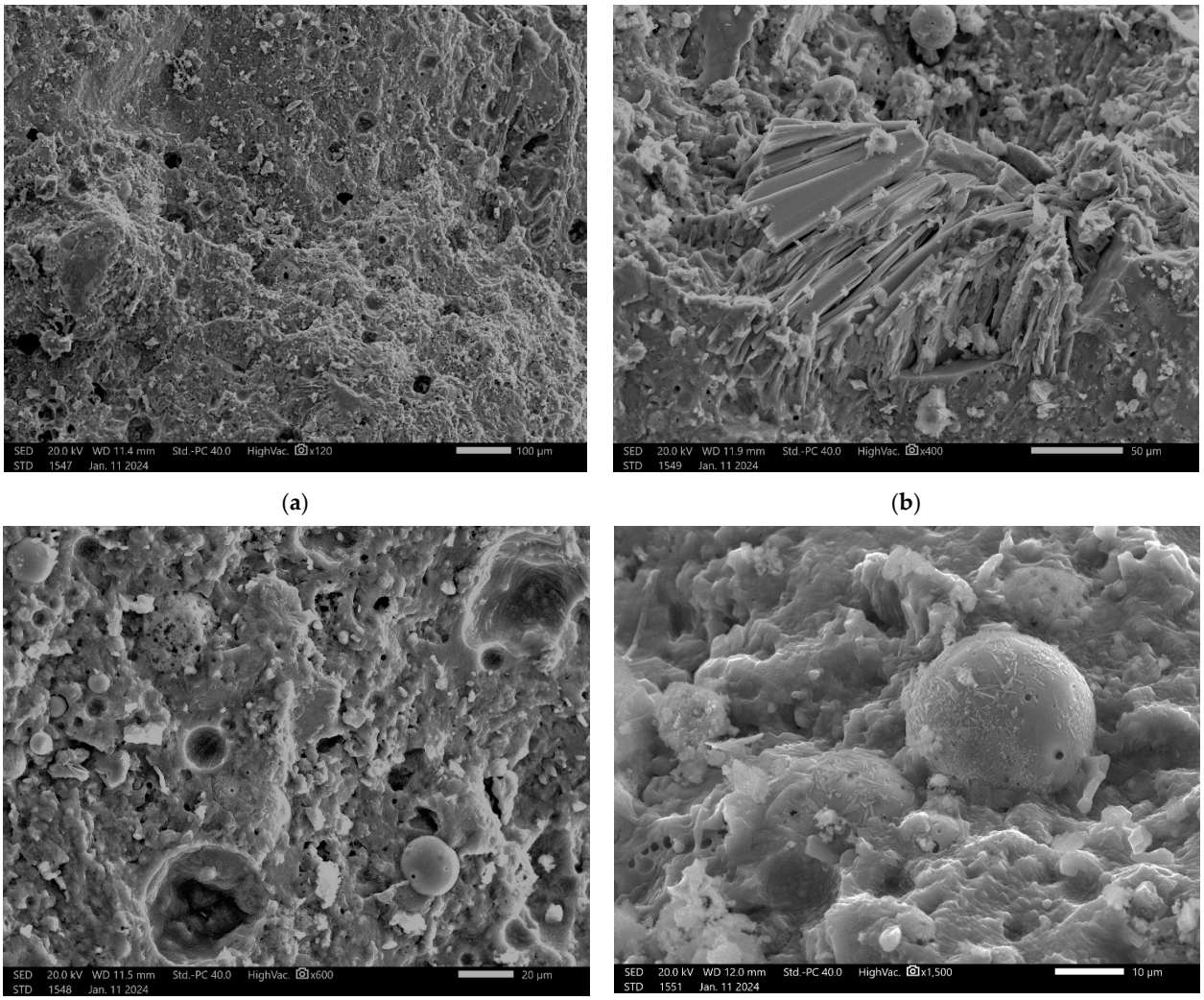

Figure 10. SEM images of geopolymer composite: (**a**) magnification 120×; (**b**) magnification 400×; (**c**) magnification 600×; (**d**) magnification 1500×.

The observed matrix is typical of geopolymer materials [60,61]. At a large magnification, undissolved particles from fly ash with a spherical shape can be observed (Figure 10). There is no incoherence or agglomeration of the additives visible in the matrix.

For the selected point, EDS analysis is also provided (Figure 11 and Table 9).

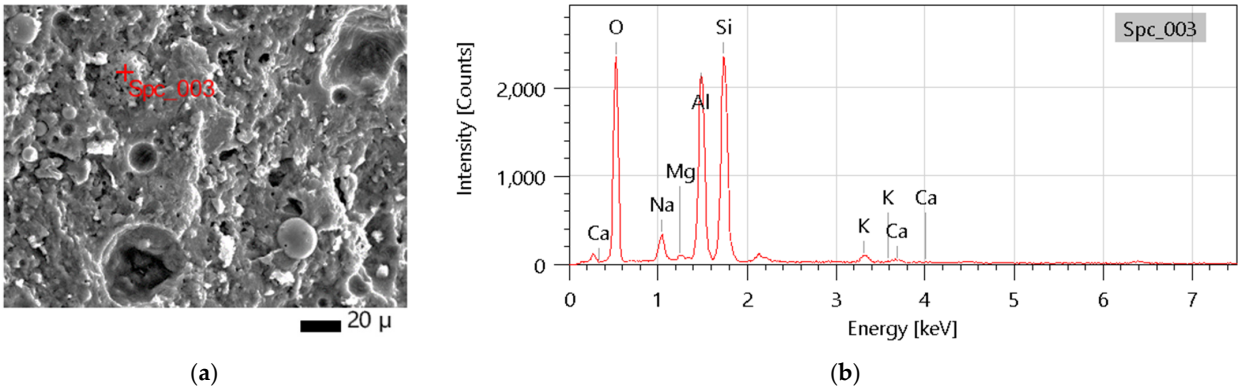

Figure 11. EDS analysis for the selected point of the geopolymer composite: (**a**) SEM figure with specific points selected for analysis; (**b**) plot with information about peaks for particular elements.

Table 9. Oxide composition from EDS analysis.

Oxide Composition	Mass wt. %	Molar Ratio [%]
Na_2O	5.61 ± 0.25	6.39 ± 0.28
MgO	0.66 ± 0.09	1.16 ± 0.17
Al_2O_3	35.41 ± 0.58	24.52 ± 0.40
SiO_2	55.88 ± 0.85	65.65 ± 1.00
K_2O	1.55 ± 0.12	1.16 ± 0.09
CaO	0.89 ± 0.10	1.13 ± 0.13

The composition presented in Table 9 is in line with the investigation performed for the raw materials and the typical composition of geopolymers [40]. The main ingredients are SiO_2 and Al_2O_3, which build the main structure of the materials. The analysis did not show any compounds of iron, but it has to be stressed that EDS is a qualitative not quantitative analysis, and it was performed only for one point. The presence of Na_2O is an effect of activation by solutions with this ingredient.

In Figure 12, the mineralogical composition of the geopolymer composite is presented.

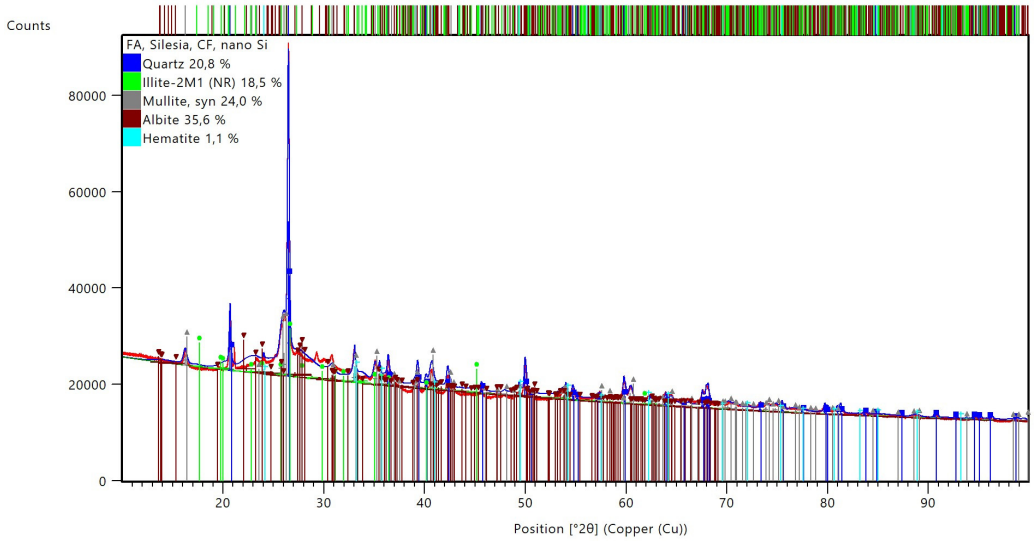

Figure 12. XRD patterns of the geopolymer composite.

Compared to the raw materials, some minerals were still present in the composition, including quartz, mullite, and hematite. The difference in their proportion is due to a method that shows only the composition of the crystalline phase. In the geopolymer composition, new phases are also visible. These are illite and albite. The occurrence of illite is a result of the transformation of muscovite, which is a component of coal shale [62]. The presence of albite is an effect of the interaction of Si-O and Al-O monomers with the alkaline activators [63,64]. Also, it should be noted that anhydrite, which is a component of fly ash and coal shale, is not visible in the geopolymer composition. It is an effect of the dissolution of this phase in the alkaline medium to form the subsequent geopolymer network [62]. The phases present in the raw materials transformed to create new crystalline components visible in the XRD patterns, as well as an amorphous geopolymer network that is not visible using this kind of analysis.

4. Discussion and Future Studies

The preliminary results show the high relevance of the properties of the geopolymer composition for road applications. Information about the obtained results and a comparison with basic requirements are presented in Table 10.

Table 10. Key properties of geopolymers for road applications.

No	Investigated Parameter	Results	Advantages in Road Construction
1	Density	1.53 g/cm^3	There are a lack of formal requirements. Relatively low density is an advantage for pre-casting elements for pavements.
2	Compressive strength	37.70 MPa	The compressive strength determines the class of road where the material can be used. There are possible applications in maneuvering areas, storage areas, for making road surfaces, sidewalks, access roads, and parking lots.
3	Abrasion resistance	The test shows low abrasion resistance.	There are a lack of formal requirements. Low abrasion resistance is connected to longer predicted time of road usage.
4	Freeze–thaw resistance	The results suggest that the material should be resistant for a minimum of 10 years	The minimum period for road usage is fulfilled. Further tests are required.
5	Salt resistance	Preliminary tests suggest resistance against salt.	There are a lack of formal requirements. However, from a practical point of view, the materials must be resistant against salt used as an anti-slip layer during the winter.
6	Microstructure	Typical structure for a geopolymer material.	A geopolymer material should be durable in different conditions. Further tests are required.
7	Chemical composition	Mainly silica and aluminia. There are a lack of hazardous elements	The material has the potential to be safe for the environment. Further tests are required.
8	Mineralogical composition	Albite, mullite, illite, quartz	There is a lack of regulation. Minerals should be considered safe for the environment.

In the case of scaling up this technology for practical application, further investigation is required. The most important area of research should include the following aspects.

- Environmental safety, including leaching tests for ready compositions; despite the raw materials not showing hazardous components, environmental safety should be additionally confirmed before further applications.
- Additional research for material durability, also in corrosive environments and on the polluted surface, as well as reactions with carbon dioxide; the surface has to be resistant to the most popular pollutants on the road, i.e., those associated with acid rain and other elements that potentially can appear on the road, including oils.
- Long-term cracking resistance—freeze–thaw studies should be continued for longer periods, e.g., for 25 years. Additionally, there should be experiments with extreme cold or high humidity.

The above tests should be carried out before the first stage of scalability and real-world applications on a medium scale. Next steps may involve improving compositions with additional components, such as nano-titanium dioxide, which can be applied to obtain other desired properties, including photocatalytic ones. Also, before application on a wider scale, technology has to be improved, as well as the process of production. There are also some limitations connected to wider applications of geopolymers, including a lack of

proper standards for these materials, which can make practical application on a wider scale (beyond experimental installations) difficult.

5. Conclusions

A new material dedicated to road application has been synthesized and investigated. The most important results are as follows.

- The chemical composition (elemental and oxide) of the final composition is in line with investigations performed for raw materials and typical compositions of geopolymers. The main ingredients are SiO_2 and Al_2O_3, which build the main structure of the material.
- The mineralogical composition is a geopolymer material based on quartz, mullite, and hematite that is not transformed during the geopolymerization process, alongside other components, such as illite and albite, that are the results of the manufacturing process.
- The additives allow for a reduction in the weight of the composition from 1.78 to 1.53 g/cm^3.
- The compressive strength of the investigated paste is almost 35 MPa for the reference sample and almost 38 MPa for the reference sample. The addition of fine aggregate or coarse aggregate can increase the value of this composition.
- The additives improve the abrasion resistance of geopolymers. Compared to the reference samples, a lower mass loss was noted.
- The additives enhance the freeze–thaw resistance of the geopolymers.
- Visual observation of samples with a salt layer showed that salt does not significantly influence the structure of the material.
- Microstructure investigation showed a structure typical of geopolymer materials. At a large magnification, in the structure, we observed some undissolved particles which came from fly ash. No incoherence or agglomeration of the additives was visible in the matrix.

The preliminary results show the high relevance of the properties of geopolymer compositions for road applications. However, for practical applications, further investigations are required to confirm the environmental safety of the material in leaching tests, alongside additional research on material durability. Moreover, material synthesis with the usage of additional components, such as nano-titanium dioxide, can be applied to obtain other desired properties, including photocatalytic ones.

Author Contributions: Conceptualization, K.K.; methodology, K.K. and M.Ł.; validation, B.F., M.Ł. and L.A.; formal analysis, A.K.; investigation, A.K. and B.F.; resources, K.K. and M.Ł.; data curation, A.K.; writing—original draft preparation, A.K. and K.K.; writing—review and editing, L.A.; visualization, A.K. and B.F.; supervision, K.K.; project administration, K.K.; funding acquisition, K.K. All authors have read and agreed to the published version of the manuscript.

Funding: This research was funded by the project titled "Development of geopolymer composites as a material for protection of hazardous wrecks and other critical underwater structures against corrosion" under the M-ERA.NET 3 program by the Polish National Centre for Research and Development, grant number M-ERA.NET3/2021/71/MAR-WRECK/2022.

Data Availability Statement: The original contributions presented in the study are included in the article; further inquiries can be directed to the corresponding author.

Conflicts of Interest: The authors declare no conflicts of interest. The funders had no role in the design of the study; in the collection, analyses, or interpretation of data; in the writing of the manuscript; or in the decision to publish the results.

Abbreviations

The following abbreviations are used in this manuscript:

EDS	Energy-dispersive X-ray spectroscopy
SEM	Scanning electron microscopy
XRD	X-ray diffraction
XRF	X-ray fluorescence
XRF	X-ray fluorescence

References

1. Belaïd, F. How Does Concrete and Cement Industry Transformation Contribute to Mitigating Climate Change Challenges? *Resour. Conserv. Recycl. Adv.* **2022**, *15*, 200084. [CrossRef]
2. Barbhuiya, S.; Kanavaris, F.; Das, B.B.; Idrees, M. Decarbonising Cement and Concrete Production: Strategies, Challenges and Pathways for Sustainable Development. *J. Build. Eng.* **2024**, *86*, 108861. [CrossRef]
3. Mohd Tahir, M.F.; Abdullah, M.M.A.B.; Abd Rahim, S.Z.; Mohd Hasan, M.R.; Saafi, M.; Putra Jaya, R.; Mohamed, R. Potential of Industrial By-Products Based Geopolymer for Rigid Concrete Pavement Application. *Constr. Build. Mater.* **2022**, *344*, 128190. [CrossRef]
4. Sharma, U.; Gupta, N.; Saxena, K.K. Comparative Study on the Effect of Industrial By-Products as a Replacement of Cement in Concrete. *Mater. Today Proc.* **2021**, *44*, 45–51. [CrossRef]
5. Rihan, M.A.M.; Onchiri, R.O.; Gathimba, N.; Sabuni, B. Mix Design Approaches of Eco-Friendly Geopolymer Concrete: A Critical Review. *Hybrid Adv.* **2024**, *7*, 100290. [CrossRef]
6. Cong, P.; Du, R.; Gao, H.; Chen, Z. Comparison and Assessment of Carbon Dioxide Emissions between Alkali-Activated Materials and OPC Cement Concrete. *J. Traffic Transp. Eng. (Engl. Ed.)* **2024**, *11*, 918–938. [CrossRef]
7. Shi, C.; Zhao, R.; Wang, W.; Zhang, S. Effect of Load on Bonding Properties and Salt Freeze-Thaw Resistance of Bridge Expansion Joint Concrete. *Constr. Build. Mater.* **2024**, *411*, 134680. [CrossRef]
8. Korniejenko, K.; Nykiel, M.; Choinska, M.; Jexembayeva, A.; Konkanov, M.; Aruova, L. An Overview of Micro- and Nano-Dispersion Additives for Asphalt and Bitumen for Road Construction. *Buildings* **2023**, *13*, 2948. [CrossRef]
9. Qin, Z.; Yuan, Y.; Chen, Z.; Li, Y.; Xia, Y. Combined Preparation and Application of Geopolymer Pavement Materials from Coal Slurry-Slag Powder-Fly Ash Mining Solid Waste: A Case Study. *Constr. Build. Mater.* **2024**, *441*, 137510. [CrossRef]
10. Azad, N.M.; Samarakoon, S.M.S.M.K. Utilization of Industrial By-Products/Waste to Manufacture Geopolymer Cement/Concrete. *Sustainability* **2021**, *13*, 873. [CrossRef]
11. Korniejenko, K.; Halyag, N.; Mucsi, G. Fly Ash as a Raw Material for Geopolymerisation—Chemical Composition and Physical Properties. *IOP Conf. Ser. Mater. Sci. Eng.* **2019**, *706*, 012002. [CrossRef]
12. Al Biajawi, M.I.; Embong, R.; Muthusamy, K.; Ismail, N.; Obianyo, I.I. Recycled Coal Bottom Ash as Sustainable Materials for Cement Replacement in Cementitious Composites: A Review. *Constr. Build. Mater.* **2022**, *338*, 127624. [CrossRef]
13. Zeng, Y.; Chen, Y.; Liu, Y.; Wu, T.; Zhao, Y.; Jin, D.; Xu, F. Prediction of Compressive and Flexural Strength of Coal Gangue-Based Geopolymer Using Machine Learning Method. *Mater. Today Commun.* **2025**, *44*, 112076. [CrossRef]
14. Min, W.; Jin, W.; He, X.; Wu, R.; Chen, K.; Chen, J.; Xia, J. Experimental Study on the Flexural Fatigue Performance of Slag/Fly Ash Geopolymer Concrete Reinforced with Modified Basalt and PVA Hybrid Fibers. *J. Build. Eng.* **2024**, *94*, 109917. [CrossRef]
15. Rashad, A.M. Effect of Steel Fibers on Geopolymer Properties—The Best Synopsis for Civil Engineer. *Constr. Build. Mater.* **2020**, *246*, 118534. [CrossRef]
16. Wang, T.; Fan, X.; Gao, C.; Qu, C.; Liu, J.; Yu, G. The Influence of Fiber on the Mechanical Properties of Geopolymer Concrete: A Review. *Polymers* **2023**, *15*, 827. [CrossRef]
17. Sharma, U.; Gupta, N.; Bahrami, A.; Özkılıç, Y.O.; Verma, M.; Berwal, P.; Althaqafi, E.; Khan, M.A.; Islam, S. Behavior of Fibers in Geopolymer Concrete: A Comprehensive Review. *Buildings* **2024**, *14*, 136. [CrossRef]
18. Zhang, D.; Vitse, J.; Vandeginste, V.; Yang, Q.; Li, J. Study on the Fracture Performance of Carbon Fiber Reinforced Recycled Powder-Based Geopolymer Composites. In Proceedings of the RILEM Spring Convention and Conference 2024, Milan, Italy, 10–12 April 2024; Ferrara, L., Muciaccia, G., Trochoutsou, N., Eds.; RILEM Bookseries. Springer Nature: Cham, Switzerland, 2025; Volume 55, pp. 71–79, ISBN 978-3-031-70276-1.
19. Shafabakhsh, G.A.; Sadeghnejad, M.; Ahoor, B.; Taheri, E. Laboratory Experiment on the Effect of Nano SiO2 and TiO2 on Short and Long-Term Aging Behavior of Bitumen. *Constr. Build. Mater.* **2020**, *237*, 117640. [CrossRef]
20. Golestani, B.; Nam, B.H.; Moghadas Nejad, F.; Fallah, S. Nanoclay Application to Asphalt Concrete: Characterization of Polymer and Linear Nanocomposite-Modified Asphalt Binder and Mixture. *Constr. Build. Mater.* **2015**, *91*, 32–38. [CrossRef]
21. Filippi, S.; Cappello, M.; Merce, M.; Polacco, G. Effect of Nanoadditives on Bitumen Aging Resistance: A Critical Review. *J. Nanomater.* **2018**, *2018*, 2469307. [CrossRef]

22. Jin, H.; Lee, T.M.; Choi, H.; Kim, K.-S. Effects of Process Variables for NO Conversion by Double-Layered Photocatalytic Mortar with TiO_2 Nanoparticles. *J. Ind. Eng. Chem.* **2023**, *117*, 461–472. [CrossRef]
23. Bhat, F.S.; Mir, M.S. Performance Evaluation of Nanosilica-Modified Asphalt Binder. *Innov. Infrastruct. Solut.* **2019**, *4*, 63. [CrossRef]
24. Amini, A.; Ziari, H.; Saadatjoo, S.A.; Hashemifar, N.S.; Goli, A. Rutting Resistance, Fatigue Properties and Temperature Susceptibility of Nano Clay Modified Asphalt Rubber Binder. *Constr. Build. Mater.* **2021**, *267*, 120946. [CrossRef]
25. Tan, Y.; Xie, J.; Wang, Z.; Li, K.; He, Z. Effect of Halloysite Nanotubes (HNTs) and Organic Montmorillonite (OMMT) on the Performance and Mechanism of Flame Retardant-Modified Asphalt. *J. Nanopart. Res.* **2023**, *25*, 74. [CrossRef]
26. Karnati, S.R.; Oldham, D.; Fini, E.H.; Zhang, L. Surface Functionalization of Silica Nanoparticles to Enhance Aging Resistance of Asphalt Binder. *Constr. Build. Mater.* **2019**, *211*, 1065–1072. [CrossRef]
27. Debbarma, K.; Debnath, B.; Sarkar, P.P. A Comprehensive Review on the Usage of Nanomaterials in Asphalt Mixes. *Constr. Build. Mater.* **2022**, *361*, 129634. [CrossRef]
28. Yi, C.; Boluk, Y.; Bindiganavile, V. Preparation of Geopolymers with Nanosilica and Water-in-Air Pickering Emulsion: Mechanisms Underlying Its Rheology, Polymerization, and Strength. *Langmuir* **2024**, *40*, 11436–11449. [CrossRef]
29. Ahmed, H.U.; Mohammed, A.S.; Mohammed, A.A. Engineering Properties of Geopolymer Concrete Composites Incorporated Recycled Plastic Aggregates Modified with Nano-Silica. *J. Build. Eng.* **2023**, *75*, 106942. [CrossRef]
30. Vanitha, N.; Revathi, T.; Jeyalakshmi, R. Influence on Rheology and Microstructure of Nanosilica and Modified Polycarboxylate in Water-Glass-Activated Fly Ash/Ground Granulated Blast Furnace Slag Geopolymers. *ChemistrySelect* **2023**, *8*, e202203491. [CrossRef]
31. Hashemi, A.; Mousavi, S.S.; Nazarpour, H.; Dehestani, M. Effect of Nano-SiO_2 and Sulfate Solutions Curing on Bond Strength of GGBFS-Based Geopolymer Repairing Mortar. *Constr. Build. Mater.* **2024**, *435*, 136778. [CrossRef]
32. Shi, J.; Shen, Y.; Zhang, W.; Fu, Y.; Kong, X. Effects of Three Different Nanomaterials on the Properties and Microstructure of Sludge Based Geopolymers. *Constr. Build. Mater.* **2024**, *414*, 134965. [CrossRef]
33. Drabczyk, A.; Kudłacik-Kramarczyk, S.; Korniejenko, K.; Figiela, B.; Furtos, G. Review of Geopolymer Nanocomposites: Novel Materials for Sustainable Development. *Materials* **2023**, *16*, 3478. [CrossRef] [PubMed]
34. Khater, H.M.; Gharieb, M. Synergetic Effect of Nano-Silica Fume for Enhancing Physico-Mechanical Properties and Thermal Behavior of MK-Geopolymer Composites. *Constr. Build. Mater.* **2022**, *350*, 128879. [CrossRef]
35. Peturai, P.; Sanguanpak, S.; Chiemchaisri, C.; Chiemchaisri, W.; Lu, M.C. Photocatalytic Removals of Imidacloprid Insecticide in TiO_2- and Fe_2O_3-Immobilized Porous Geopolymer Granules. *Chemosphere* **2024**, *362*, 142940. [CrossRef]
36. Shumuye, E.D.; Mehrpay, S.; Fang, G.; Li, W.; Wang, Z.; Uge, B.U.; Liu, C. Influence of Novel Hybrid Nanoparticles as a Function of Admixture on Responses of Engineered Geopolymer Composites: A Review. *J. Build. Eng.* **2024**, *86*, 108782. [CrossRef]
37. Ünal, M.T.; Gökçe, H.S.; Ayough, P.; Alnahhal, A.M.; Şimşek, O.; Nehdi, M.L. Nanomaterial and Fiber-Reinforced Sustainable Geopolymers: A Systematic Critical Review. *Constr. Build. Mater.* **2023**, *404*, 133325. [CrossRef]
38. Alterary, S.S.; Marei, N.H. Fly Ash Properties, Characterization, and Applications: A Review. *J. King Saud Univ. Sci.* **2021**, *33*, 101536. [CrossRef]
39. Wardhono, A. Comparison Study of Class F and Class C Fly Ashes as Cement Replacement Material on Strength Development of Non-Cement Mortar. *IOP Conf. Ser. Mater. Sci. Eng.* **2018**, *288*, 012019. [CrossRef]
40. Bazan, P.; Figiela, B.; Kozub, B.; Łach, M.; Mróz, K.; Melnychuk, M.; Korniejenko, K. Geopolymer Foam with Low Thermal Conductivity Based on Industrial Waste. *Materials* **2024**, *17*, 6143. [CrossRef]
41. Stefanini, L.; Ansari, D.; Walkley, B.; Provis, J.L. Characterisation of Calcined Waste Clays from Kaolinite Extraction in Alkali-Activated GGBFS Blends. *Mater. Today Commun.* **2024**, *38*, 107777. [CrossRef]
42. Deng, Y.; Zhang, Z.; Hu, J.; Yu, Q.; Shi, C. Fundamental Study on Reactive Components and Leaching Kinetics of Ceramic Waste for Geopolymer Production. *Compos. Part B Eng.* **2025**, *295*, 112211. [CrossRef]
43. Saini, G.; Vattipalli, U. Assessing Properties of Alkali Activated GGBS Based Self-Compacting Geopolymer Concrete Using Nano-Silica. *Case Stud. Constr. Mater.* **2020**, *12*, e00352. [CrossRef]
44. Thatikonda, N.; Mallik, M.; Rao, S.V.; Dubey, S. Performance and Microstructural Characterization of Sustainable Self-Compacting Geopolymer Concrete with Multi-Component Binders. *Sustain. Chem. Pharm.* **2025**, *44*, 101926. [CrossRef]
45. Korniejenko, K.; Łach, M.; Marczyk, J.; Ziejewska, C.; Halyag, N.; Mucsi, G. Fly Ash as a Raw Material for Geopolymerisation-Mineralogical Composition and Morphology. *IOP Conf. Ser. Mater. Sci. Eng.* **2019**, *706*, 012006. [CrossRef]
46. El Khomsi, A.; Gharzouni, A.; Sobrados, I.; Bourbon, X.; Michau, N.; Rossignol, S. A MAS-NMR Analysis of 29Si, 27Al and 1H on the Temperature's Impact on Geopolymer Grouts Derived from Argillite and Metakaolin. *J. Non-Cryst. Solids* **2024**, *642*, 123163. [CrossRef]
47. Knauss, K.G.; Thomas, J.W. Muscovite Dissolution Kinetics as a Function of pH and Time at 70 °C. *Geochim. Cosmochim. Acta* **1989**, *53*, 1493–1501. [CrossRef]
48. Guo, L.; Liu, J.; Zhou, M.; An, S. Effect of an Alkali Activators on the Compressive Strength and Reaction Mechanism of Coal Gangue-Slag-Fly Ash Geopolymer Grouting Materials. *Constr. Build. Mater.* **2024**, *426*, 136012. [CrossRef]

49. Ziejewska, C.; Bąk, A.; Hodor, K.; Hebda, M. Eco-Friendly Coal Gangue and/or Metakaolin-Based Lightweight Geopolymer with the Addition of Waste Glass. *Materials* **2023**, *16*, 6054. [CrossRef]
50. *EN 12390-3:2019*; Testing of Concrete—Part 3: Compressive Strength of Test Specimens. Polski Komitet Normalizacyjny: Warsaw, Poland, 2020.
51. Klimada 2.0. Available online: https://klimada2.ios.gov.pl/liczba-dni-z-przejsciem-przez-0-c/ (accessed on 11 February 2025).
52. John, S.K.; Nadir, Y.; Girija, K. Effect of Source Materials, Additives on the Mechanical Properties and Durability of Fly Ash and Fly Ash-Slag Geopolymer Mortar: A Review. *Constr. Build. Mater.* **2021**, *280*, 122443. [CrossRef]
53. Shehata, N.; Mohamed, O.A.; Sayed, E.T.; Abdelkareem, M.A.; Olabi, A.G. Geopolymer Concrete as Green Building Materials: Recent Applications, Sustainable Development and Circular Economy Potentials. *Sci. Total Environ.* **2022**, *836*, 155577. [CrossRef]
54. Sizirici, B.; Fseha, Y.; Cho, C.-S.; Yildiz, I.; Byon, Y.-J. A Review of Carbon Footprint Reduction in Construction Industry, from Design to Operation. *Materials* **2021**, *14*, 6094. [CrossRef] [PubMed]
55. Aminzadegan, S.; Shahriari, M.; Mehranfar, F.; Abramović, B. Factors Affecting the Emission of Pollutants in Different Types of Transportation: A Literature Review. *Energy Rep.* **2022**, *8*, 2508–2529. [CrossRef]
56. Korniejenko, K.; Łach, M.; Mikuła, J. The Influence of Short Coir, Glass and Carbon Fibers on the Properties of Composites with Geopolymer Matrix. *Materials* **2021**, *14*, 4599. [CrossRef] [PubMed]
57. Kuna, E.; Bögöly, G. Overview of Mechanical Degradation of Aggregates, Related Standards, and the Empirical Relations of the Parameters. *Bull. Eng. Geol. Environ.* **2024**, *83*, 274. [CrossRef]
58. Bibitha, L.; Durgalakshmi, S.; Athiappan, K. Evaluation of Strength, Wear, and Skid Resistance in Pavement Quality Concrete with Partial Replacement of Steel Slag. *Matéria* **2025**, *30*, e20240636. [CrossRef]
59. Luhar, S.; Luhar, I.; Gupta, R. Durability Performance Evaluation of Green Geopolymer Concrete. *Eur. J. Environ. Civ. Eng.* **2022**, *26*, 4297–4345. [CrossRef]
60. Yalcinkaya, B.; Spirek, T.; Bousa, M.; Louda, P.; Růžek, V.; Rapiejko, C.; Buczkowska, K.E. Unlocking the Potential of Biomass Fly Ash: Exploring Its Application in Geopolymeric Materials and a Comparative Case Study of BFA-Based Geopolymeric Concrete against Conventional Concrete. *Ceramics* **2023**, *6*, 1682–1704. [CrossRef]
61. Kozub, B.; Dudek, J.; Melnychuk, M. The Effect of Oil Additives on the Properties of Fly Ash-Based Foamed Geopolymers. *Materials* **2024**, *17*, 5819. [CrossRef]
62. Tome, S.; Nana, A.; Tchakouté, H.K.; Temuujin, J.; Rüscher, C.H. Mineralogical Evolution of Raw Materials Transformed to Geopolymer Materials: A Review. *Ceram. Int.* **2024**, *50*, 35855–35868. [CrossRef]
63. Chuewangkam, N.; Kidkhunthod, P.; Pinitsoontorn, S. Direct Evidence for the Mechanism of Early-Stage Geopolymerization Process. *Case Stud. Constr. Mater.* **2024**, *21*, e03539. [CrossRef]
64. Xu, X.; Bao, S.; Zhang, Y.; Luo, Y.; Qin, L.; Li, S. Role of Particle Fineness and Reactive Silicon-Aluminum Ratio in Mechanical Properties and Microstructure of Geopolymers. *Constr. Build. Mater.* **2021**, *313*, 125483. [CrossRef]